EXPERIMENTAL STUDY ON HEAT TRANSFER PERFORMANCE OF NANOFLUID COOLING UNDER HIGH HEAT FLUX DENSITY

Haifei Chen*[*1], Yanglong Zhao[1], Hao Wang[1], Yangyang Zhu[1], Tao Hong, [1],Yunjie Wang[2]

[*1]Engineering Laboratory for High-Value Utilization of Biomass Waste in Petroleum and Chemical Industries, Changzhou University, Changzhou, Jiangsu Province, China

[2]School of Energy and Power Engineering, Nanjing University of Science and Technology, Nanjing 210094, Jiangsu Province, China

[*] Corresponding author; E-mail: chenhaifei6@163.com

High-power devices such as fast-charging equipment for new energy vehicles and laser technologies may experience efficiency degradation or even damage due to overheating during operation, making high heat flux cooling technologies a research focus. To address the limited heat-carrying capacity of traditional cooling media, the cooling performance of TiO_2 nanofluids under high heat flux conditions was investigated, and a heat transfer experimental test platform under high heat flux density of spray cooling was established. The effects of TiO_2 mass fraction, spray flow rate, and heating power on cooling performance are examined. The results demonstrate that the 0.1 wt% TiO_2 nanofluid achieves the optimal performance, with a heat transfer coefficient of 3.59 W/cm²·K. Higher mass fractions lead to increased viscosity and particle interactions, reducing heat transfer efficiency. Furthermore, increasing the spray flow rate enhances cooling performance, but higher TiO_2 concentrations lead to reduced performance due to particle deposition on the heat source surface. The TiO_2 nanofluids exhibit significant advantages under high heat flux density. Surface temperature of 25.3°C, at a heating power of 500 W, can be maintained with 0.1 wt% TiO_2 nanofluid. This research provides valuable insights for optimizing the use of TiO_2 nanofluids in high heat flux density applications.

Key words*: high heat flux, nanofluid, cooling technology, heat transfer performance*

1. Introduction

With rapid development of high-power devices, such as fast-charging equipment for new energy vehicles, laser technologies, and other advanced technologies, the challenge of thermal management has become increasingly critical [1]. Especially in high heat flux density applications, traditional heat dissipation methods, such as air cooling and water cooling, have been unable to meet the extremely high heat dissipation requirements. Excessive heat flux will cause the device surface to overheat, resulting in system performance degradation and adversely affecting the stability and life of the system

[2,3]. Therefore, the exploration of advanced and efficient cooling solutions is essential to ensure optimal performance and long-term reliability.

Among various cooling techniques, spray cooling stands out due to its advantages in heat resistance, temperature uniformity, rapid response, and cooling efficiency [4]. Li *et al.* [5] demonstrated the viability of spray cooling in dissipating heat in high heat flux density applications. Liu *et al.* [6] studied the impact of ambient pressure on spray cooling in a closed-loop system. At 0.4 MPa, the critical heat flux reached 122 W/cm², with a surface temperature of 56°C and a heat transfer coefficient of 2.1 W/cm²·K.

Traditional spray cooling systems, although effective for basic heat dissipation, encounter considerable limitations when used in high-load, high-heat-flux-density environments. Conventional cooling medium, such as water and ethanol, have inherent limitations due to their thermal properties and phase change characteristics [7]. These limitations hinder the ability to achieve rapid and efficient cooling, making it challenging to meet the cooling requirements of high-power devices. Tian *et al.* [8] found that an ethanol-R141b blend used in electro-spray cooling produced a heat transfer coefficient of only 1.9 W/cm²·K under optimal conditions.

The introduction of nanofluids has significantly improved the thermal performance of traditional base fluids, making them a promising coolant for various applications [9,10]. Maly *et al.* [11] indicated that the nanoparticles enhance spray cooling performance mainly by altering the thermal properties, without significantly affecting fluid dynamics or spray characteristics. Hsieh *et al.* [12] tested seven nanofluids and found that their heat transfer coefficients exceeded that of water under nucleate boiling and critical heat flux conditions. Performance improved with increasing volume fraction, reaching optimal results at a 0.1% concentration, where the critical heat flux density was 375 W/cm².

To address the challenges of overheating, reduce heat loss, and overcome the limited heat-carrying capacity of traditional cooling fluids under high heat flux density conditions, this study investigates the spray cooling performance of TiO_2 nanofluids. Firstly, the preparation process of TiO_2 nanofluid was introduced, followed by the establishment of a high heat flux density spray cooling heat transfer experimental test platform. The effects of the TiO_2 nanofluid mass fraction, spray flow rate, and heating power on the heat transfer performance are systematically examined. The research reveals the specific mechanisms through which these parameters influence heat transfer performance. The findings provide valuable theoretical insights and practical guidance for optimizing the application of TiO_2 nanofluids in high heat flux density cooling systems.

2. Research methodology and theoretical analysis

2.1 Preparation of TiO_2 nanofluids

As shown in Tab. 1, TiO_2 nanoparticles possess excellent thermophysical properties, making them ideal for enhancing the thermal performance of nanofluids. Therefore, the experiment used 10-15 nm TiO_2 nanoparticles (rutile type; purity ≥ 98%; purchased from Shanghai Aladdin Biochemical Technology Co., Ltd., China). To improve the heat transfer efficiency of the nanofluid, it should possess good dispersibility, long-lasting suspension, and excellent stability. The experiment used a one-step method to prepare the TiO_2 nanofluid [13]. Fig. 1 shows the preparation process of TiO_2 nanofluid. First, a certain amount of TiO_2 nanoparticles is accurately weighed and added to DI water,

then, the mixture is placed on a magnetic stirrer and stirred for 1 hour; finally, it is placed in an ultrasonic oscillator and shaken for 1 hour to finally obtain TiO_2 nanofluid. The TiO_2 nanofluids with concentrations of 0 wt%, 0.05 wt%, 0.1 wt%, and 0.3 wt% were prepared through the above steps.

Table 1. Thermophysical properties of TiO_2 nanoparticles.

Thermophysical properties	Value
Density	4.26 g/cm^3
Melting point	1855 ℃
Boiling point	2900 ℃
Thermal conductivity	11.8 W/(m·K)

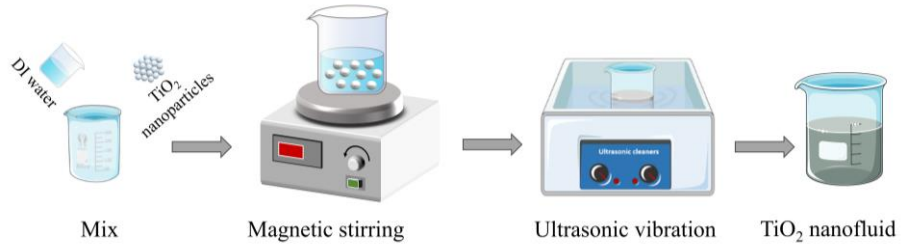

Figure 1. Preparation process of TiO_2 nanoparticles

2.2 Experimental system

To investigate the heat transfer performance of TiO_2 nanofluid spray cooling under different working conditions, a spray cooling heat transfer test bench was established. Fig. 2 and 3 show the spray cooling system, which includes three main components: the spray cooling liquid supply circulation system, simulated heat source power control system, and data acquisition system. The spray cooling liquid supply circulation system comprises a constant temperature reaction bath, filter, hydraulic pump, flow control valve, regulating rod, nozzle, connecting pipes, and valves. The simulated heat source power control system includes a heat-conductive copper block, electric heater, and power control device. The data acquisition system features a mass flowmeter, pressure sensor, K-type thermocouple, and data acquisition instrument.

The spray cooling system operates as follows. The pre-prepared nanofluid is kept in a low-temperature thermostatic reaction bath. The main circuit valve is open, and the hydraulic pump pressurizes the fluid, drawing it through a filter. The fluid is then split into two branches: one directed to the spray circuit and the other returning to the reaction bath via a pressure relief path. In the spray circuit, the fluid passes through a flow control valve and a glass rotameter before reaching the nozzle. The pressure difference atomizes the fluid into fine droplets, which impact the heated surface, transferring heat through fluid flow, evaporative convection, and nucleate boiling. The heated fluid is collected in a tank and returned to the reaction bath, completing the cycle The experimental conditions for spray cooling heat transfer experimental test platform are shown in Tab. 2.

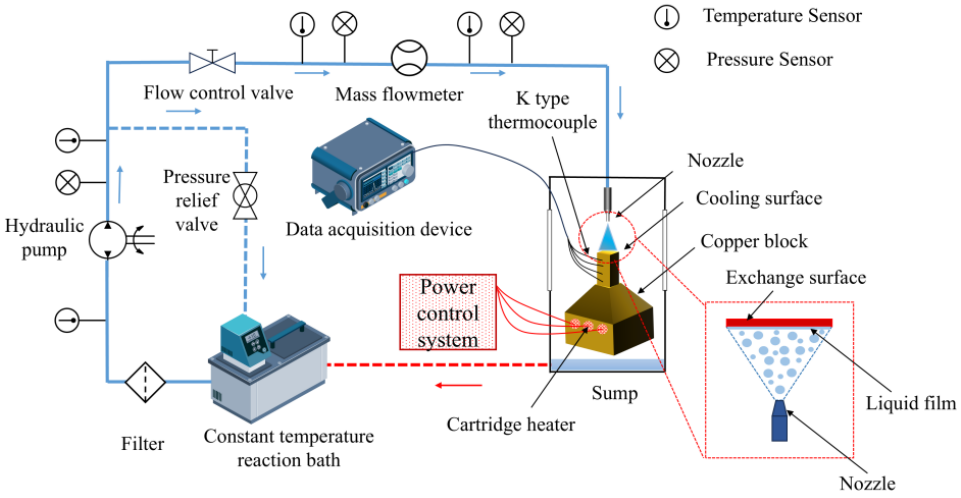

Figure 2. Flow chart of spray cooling system

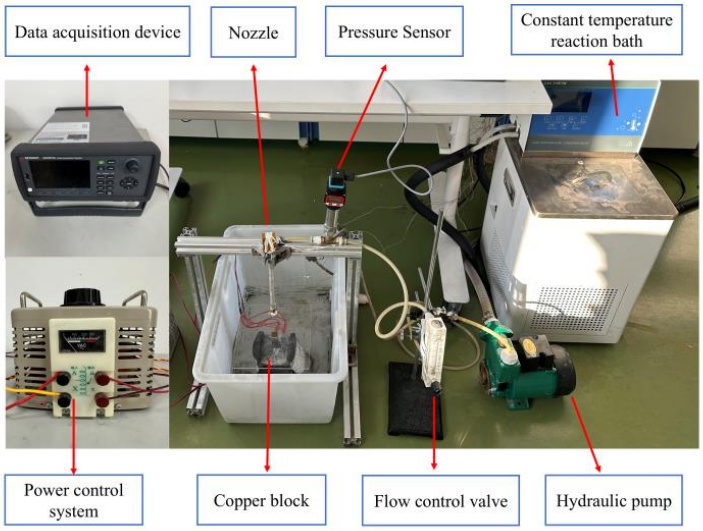

Figure 3. Spray cooling experimental system

Table 2. Spray cooling experimental conditions

Initial technical parameters	Indicator range
Nozzle height (mm)	12
Working fluid inlet temperature (℃)	15
Ambient temperature (℃)	20
Flow range (L/min)	0.6/0.8/1.0/1.2/1.4
Heating power (W)	100/200/300/400/500

2.3 Theoretical analysis

The heating block, made entirely of pure copper, is depicted in Fig. 4. The copper column is encased in a layer of rock wool insulation, with a cartridge heater installed at its base. The heat

transfer surface area of the copper column is 1 cm². K-type thermocouples are placed at four radial positions along the column at distances of 2 mm, 15 mm, 25 mm, and 35 mm from the top surface.

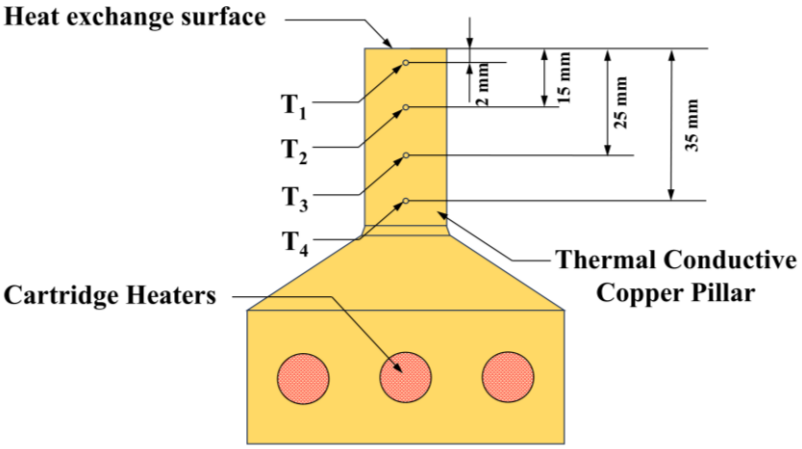

Figure 4. Schematic diagram of heating copper block structure

Due to the effective thermal insulation around the copper pillar, radial heat transfer is minimal. As a result, heat transfer in the copper pillar follows one-dimensional conduction [14]. The one-dimensional steady-state heat flux equation, derived from Fourier's law, is expressed as follows [15]:

$$q = \lambda \frac{\left(T_i - T_j\right)}{\Delta\delta} \tag{1}$$

where q is the heat flow density, λ is the thermal conductivity of the copper block, which is taken as 390 W/(m·K), T_i and T_j is the temperatures at the i-th and j-th measurement points, and $\Delta\delta$ is the distance between the two layers.

Using the one-dimensional axial temperature distribution law, the steady-state surface temperature of the copper column can be calculated as follows:

$$T_{\text{suf}} = T_1 - (T_i - T_j)\frac{\delta_1}{\Delta\delta} \tag{2}$$

where T_{suf} is the surface temperature, and T_1 is the temperature at the closest measurement point to the surface.

The heat transfer coefficient for the top surface is obtained by coupling the convective boundary condition with the heat flux boundary on the upper surface of the copper block [16]:

$$h = \frac{q}{(T_{\text{sur}} - T_{\text{in}})} \tag{3}$$

where h is the heat transfer coefficient, and T_{in} is the cooling fluid inlet temperature.

The sources of error in the experiment primarily include measurement inaccuracies and equipment inaccuracies. The main experimental equipment and accuracy are shown in Tab. 3. Therefore, the errors can be calculated according to the error propagation formula [17]:

$$\sigma_y = \sqrt{\sum_{i=0}^{n}\left(\frac{\partial f}{\partial x_i}\right)^2 \sigma_{x_i}^2} \tag{4}$$

Consequently, the errors are ±1.5% for surface temperature, ±1.1% for heat flux density, ±2.2% for heat transfer coefficient.

3. Results and discussion

3.1 Effect of TiO_2 nanofluid mass fraction on heat transfer

Fig. 5 illustrates the influence of the TiO_2 nanofluid mass fraction on the surface temperature, and heat transfer coefficient under high heat flux density. The spray cooling effect exhibits a trend of initially increasing and then decreasing as the TiO_2 nanofluid mass fraction rises. At a mass fraction of 0.1 wt%, the system achieves optimal performance, with the surface temperature reduced to 25.3°C and the heat transfer coefficient reaching 3.59 W/cm²·K. Compared to pure water, the surface temperature decreases by 6.1°C, while the heat transfer coefficient improves by 54.1%. However, at a mass fraction of 0.5 wt%, both heat transfer performance and cooling efficiency deteriorate significantly. The surface temperature increases to 32.0°C, the heat transfer coefficient declines to 2.29 W/cm²·K, and the cooling efficiency falls below the level achieved with pure water.

On the one hand, the addition of a small amount of TiO_2 nanoparticles significantly enhances the heat transfer performance of the base fluid due to the higher thermal conductivity of TiO_2 compared to pure water. Moreover, the nanoparticles undergo irregular motion under Brownian forces, which facilitate the rapid migration and dispersion of heat. However, as the mass fraction of TiO_2 nanofluid increases, the number of nanoparticles in the base fluid also increases, leading to stronger particle interactions. This, in turn, diminishes the effectiveness of Brownian motion and reduces the overall energy transfer efficiency.

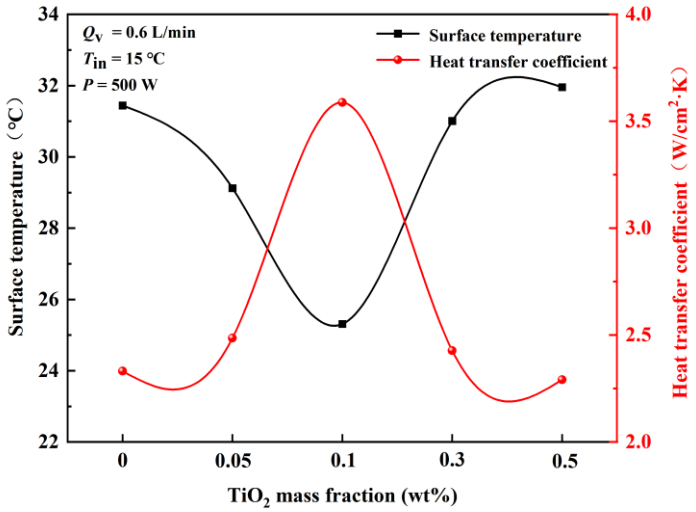

Figure 5. Surface temperature and heat transfer coefficient versus mass fraction of TiO_2 nanofluids

On the other hand, variations in the mass fraction of the nanofluid can influence its surface properties. As the mass fraction increases, the dynamic viscosity of the nanofluid rises significantly, which increases the flow resistance of the droplets on the heated surface. Simultaneously, the viscosity of the liquid film also increases, restricting the expansion and evaporation of the droplets, and ultimately impairing the heat transfer capability.

3.2 Effect of spray flow rate on heat transfer

Figs. 6 and 7 present the variations in surface temperature and heat transfer coefficient of TiO_2 nanofluids at different spray flow rates. As shown in the figures, an increase in spray flow rate leads to a gradual decrease in surface temperature and a corresponding increase in surface heat transfer coefficient. This behavior can be attributed to the increase in mass of the working fluid, which raises both the speed and number of atomized droplets from the nozzle. This, in turn, enhances the impact and disruption of droplets on the liquid film on the heat source surface, resulting in a thinner boundary layer attached to the wall and improving heat transfer efficiency.

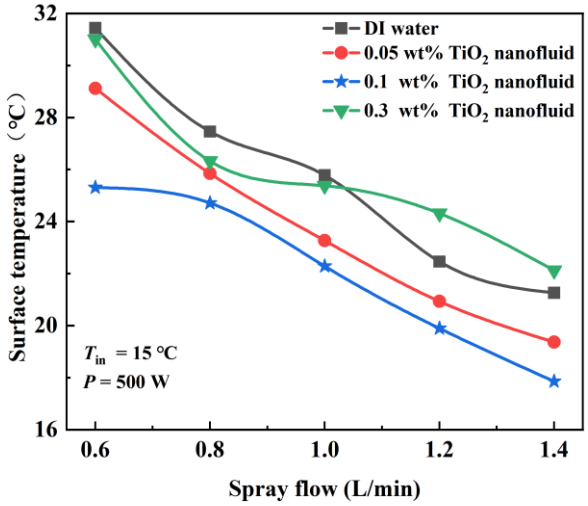

Figure 6. Surface temperature changes under different TiO_2 nanofluid spray flow rates

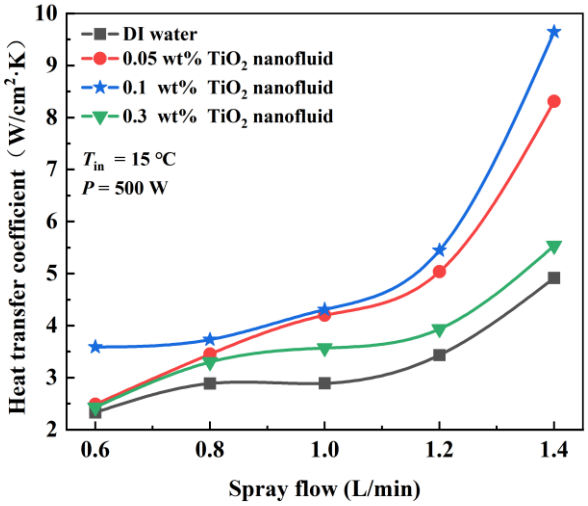

Figure 7. Heat transfer coefficient changes under different TiO_2 nanofluid spray flow rates

Specifically, at all spray flow rates, the TiO_2 nanofluid with a mass fraction of 0.1 wt% consistently exhibits the best heat transfer performance. As the spray flow rate increases from 0.8 L/min to 1.4 L/min, the surface temperature decreases by 27.5%, and the surface heat transfer coefficient increases by 158.5%. The TiO_2 nanofluid with a mass fraction of 0.05 wt% ranks second, with surface temperature reduction of 25.1% and heat transfer coefficient increase of 140.7%. The

smallest temperature reduction, 16%, was observed with the 0.3 wt% TiO_2 nanofluid, which resulted in a 67.8% increase in the heat transfer coefficient. This increase is lower than 22.5% temperature drop and 70.3% heat transfer coefficient rise observed when pure water is used as working fluid. When the spray flow rate exceeds 1.0 L/min, the surface temperature of the 0.3 wt% TiO_2 nanofluid even surpasses that of pure water, and its heat transfer coefficient approaches that of pure water.

The observed phenomenon can be explained by the fact that as the flow rate of nanofluid with higher mass fraction increases, more nanoparticles impact the heat source surface, leading to the deposition of nanoparticles on the surface. This deposition increases the heat transfer resistance and hinders the transfer of heat. In contrast, the nanofluid with a lower mass fraction has a higher inherent heat transfer coefficient, and the increase in spray flow rate exerts a flushing effect on the heat source surface, preventing excessive nanoparticle deposition and thereby enhancing the spray cooling performance.

3.3 Effect of heating power on heat transfer

Figs. 8 and 9 illustrates the trend of surface temperature and heat transfer coefficient as a function of the heating power. As shown in the figures, as the heating power increases, the surface temperatures of all three working fluids show an upward trend. However, at the same heating power, the cooling effect of nanofluids is significantly superior to that of DI water, with the TiO_2 nanofluid at a concentration of 0.1% demonstrating the best cooling performance. Specifically, as the heating power increases from 100 W to 500 W, the surface temperature of DI water rises sharply, reaching a maximum of 31.4°C, with a corresponding heat transfer coefficient increasing from 1.17 W/cm²·K to 2.33 W/cm²·K. In contrast, the surface temperatures of the TiO_2 nanofluids with concentrations of 0.05% and 0.1% are 29.1°C and 25.3°C, respectively. Their corresponding heat transfer coefficients are 2.49 W/cm²·K and 3.56 W/cm²·K, respectively. This indicates that the heat transfer advantage of nanofluid is more obvious under high heat flow conditions.

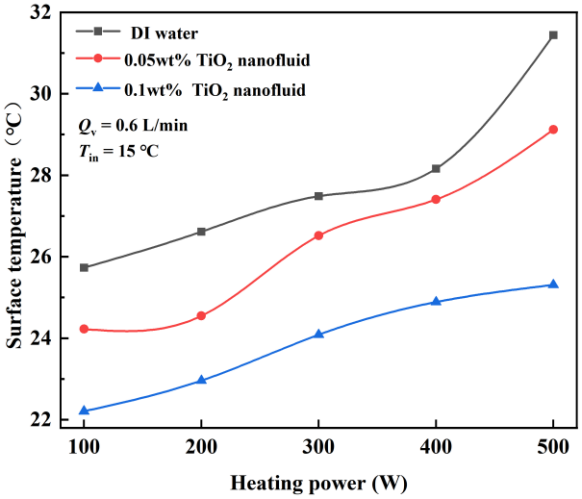

Figure 8. Surface temperature changes of TiO_2 nanofluid at different heating power

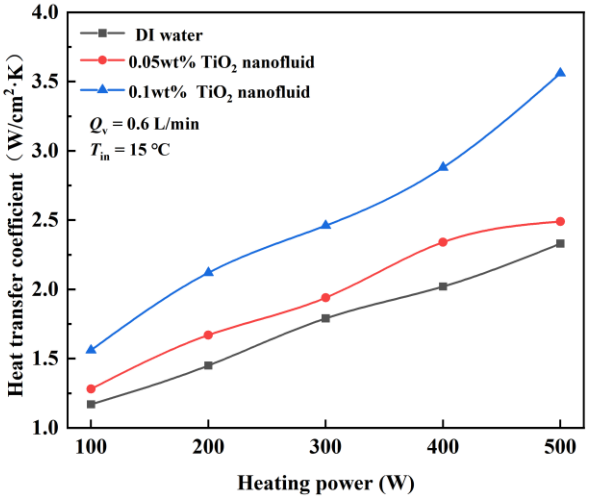

Figure 9. Heat transfer coefficient changes of TiO_2 nanofluid at different heating power

Further analysis revealed that as the heating power increases, the heat flux density gradually increases, and the main heat transfer mechanism of spray cooling shifts from convection heat transfer to evaporation heat transfer. TiO_2 nanofluid with higher concentration can adapt better to the heat dissipation needs of high heat flux density due to its significant effect in enhancing heat transfer. However, it should also be noted that too high a concentration of nanoparticles may form thermal resistance due to surface deposition, thereby affecting cooling performance.

3.4 Comparison with other cooling method

The heat transfer performance of TiO_2 nanofluid spray cooling is compared to other commonly used cooling technologies under high heat flux conditions, including fin heat sink, micro chambers, and immersion jet cooling. As shown in Fig. 10, TiO_2 nanofluid spray cooling outperforms other cooling methods in terms of heat transfer performance under high heat flux conditions, achieving the lowest surface temperature and the best heat transfer efficiency. Meanwhile, the results further highlight the effectiveness of using nanofluids as a cooling medium in enhancing the heat transfer performance of spray cooling.

From an economic perspective, the heat transfer coefficient of nanofluid spray cooling technology is increased by about 3.5W/cm²·K compared to fin heat sink with similar cost [20]. When compared to the more complex micro chambers, the heat transfer coefficient is enhanced by 3.2 W/cm²·K, while the cost is reduced by approximately 40% [21]. Therefore, nanofluid spray cooling not only offers superior cooling performance but also provides better economic efficiency. It is particularly suitable for high heat flux applications where traditional cooling methods fall short, such as fast-charging equipment for new energy vehicles and laser technologies, which require stringent surface temperature control. In these extreme thermal management scenarios, nanofluid spray cooling effectively lowers the surface temperature, ensuring the stable operation of equipment in high-temperature environments. Its outstanding heat transfer performance provides an irreplaceable advantage in high heat flux density applications.

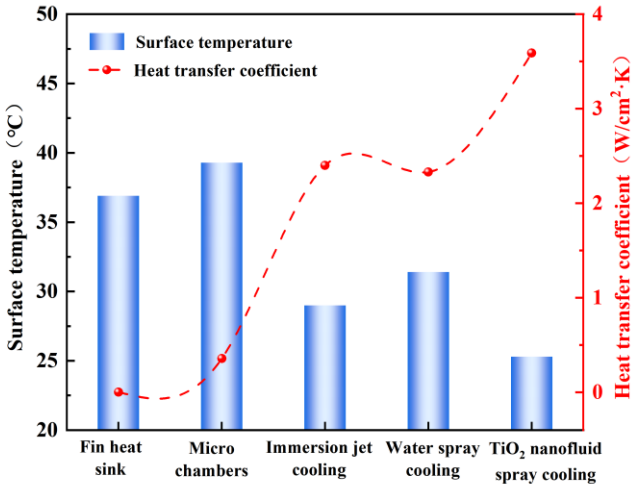

Figure 10. Comparison with other cooling method [20–22]

4. Conclusion

To address overheating issues and enhance the heat-carrying capacity of conventional cooling fluids under high heat flux density conditions, a TiO_2 nanofluid spray cooling system is proposed. This study investigates the performance of TiO_2 nanofluids as a cooling medium, focusing on the effects of TiO_2 nanofluid mass fraction, spray flow rate and heating power on cooling performance under high heat flux density. This technology is expected to provide a reference for solving the heat dissipation of high-power devices. The main conclusions are as follows:

- At different mass fractions, the 0.1 wt% TiO_2 nanofluid exhibits the best performance, with a heat transfer coefficient of 3.59 W/cm²·K. However, at higher mass fractions, increased viscosity and stronger particle interactions reduce heat transfer, resulting in lower cooling efficiency than pure water.
- Increasing the spray flow rate improves cooling by increasing droplet velocity and number, thus enhancing heat transfer. However, higher TiO_2 nanofluid mass fractions reduce heat transfer due to particle deposition on the heat source surface, which negatively affects performance and limits system improvements. Overall, 0.1 wt% TiO_2 nanofluid performs best at different flow rates.
- As the heating power increases, the surface temperature also rise. However, TiO_2 nanofluids offer significant cooling and efficiency improvements under high heat flux. The 0.1 wt% TiO_2 nanofluid performs best, maintaining a surface temperature of 25.3°C at a heating power of 500 W, showing the smallest temperature increase.

Acknowledgment

This work was sponsored by the National Natural Science Foundation of China (Grant No.51906020, 52208105), Qing Lan Project of Jiangsu Province of China, and also supported by the Project of Scientific and Technical Supporting Programs of Changzhou (Grant No. CE20235040), Practice Innovation Program of Jiangsu Province (KYCX24_3238).

Nomenclature

h - heat transfer coefficient, [W/m^2·K]
q - heat flow density, [W/m·K]
P - heating power [W]
T - temperature, [°C]

Greek symbols

λ - thermal conductivity, [W/(m·K)]
δ - distance, (mm)
Δ - difference

Subscript

i - the measurement points of the i-th layers
j - the measurement points of the j-th layers
suf - surface

References

[1] Chakraborty S., *et al*., A review on coolant selection for thermal management of electronics and implementation of multiple-criteria decision-making approach, *Applied Thermal Engineering*, (2024), 245:122807

[2] Alami AH., *et al*., Management of potential challenges of PV technology proliferation. *Sustainable Energy Technologies and Assessments*, (2022), 51:101942

[3] Hasan HA., *et al*., Experimental evaluation of thermal efficiency, electrical efficiency, and power production of low-concentrating photovoltaic-thermal system with micro-jet channel, *Applied Thermal Engineering*, (2024), 236:121526

[4] Wang Y., *et al*., A review: The development of crucial solar systems and corresponding cooling technologies, *Renewable and Sustainable Energy Reviews*, (2023), 185:113590

[5] Li Y-Y., *et al*., Theoretical study of heat transfer enhancement mechanism of high alcohol surfactant in spray cooling, *International Journal of Thermal Sciences*, (2021), 163:106816

[6] Liu J., *et al*., Influence of chamber pressure on heat transfer characteristics of a closed loop R134-a spray cooling, *Experimental Thermal and Fluid Science*, (2016), 75, pp. 89–95

[7] Chakraborty S., *et al*., A review on coolant selection for thermal management of electronics and implementation of multiple-criteria decision-making approach, *Applied Thermal Engineering*, (2024), 245:122807

[8] Tian J., *et al*., Experimental investigation on heat transfer performance during electrospray cooling with ethanol–R141b mixture, *Applied Thermal Engineering*, (2023), 230:120879

[9] Wang L, R., *et al*., A holistic and state-of-the-art review of nanotechnology in solar cells, *Sustain Energy Technol Assess*, (2022), 54:102864

[10] Sriharan G., *et al*., A review on thermophysical properties, preparation, and heat transfer enhancement of conventional and hybrid nanofluids utilized in micro and mini channel heat sink, *Sustainable Energy Technologies and Assessments*, (2023), 58:103327

[11] Malý M., *et al*., Effect of nanoparticles concentration on the characteristics of nanofluid sprays for cooling applications, *J Therm Anal Calorim*, (2019), 135, pp. 3375–3386

[12] Hsieh S-S., *et al*., Spray cooling characteristics of nanofluids for electronic power devices, *Nanoscale Res Lett*, (2015), 10:139

[13] Souza RR., *et al*., Recent advances on the thermal properties and applications of nanofluids: From nanomedicine to renewable energies, *Applied Thermal Engineering*, (2022), 201:117725

[14] Ravikumar SV., *et al.*, Enhancement of heat transfer rate in air-atomized spray cooling of a hot steel plate by using an aqueous solution of non-ionic surfactant and ethanol, *Applied Thermal Engineering*, (2014), 64, pp. 64–75

[15] Huang Y., *et al.*, Experimental study on a spray and falling-film cooling system, *Case Studies in Thermal Engineering*, (2021), 26:101057

[16] Peng H., *et al*., Thermal management of high concentrator photovoltaic system using a novel double-layer tree-shaped fractal microchannel heat sink, *Renewable Energy*, (2023), 204, pp. 77–93

[17] Chen L., *et al*., Performance evaluation of high concentration photovoltaic cells cooled by microchannels heat sink with serpentine reentrant microchannels, *Applied Energy*, (2022), 309:118478

[18] Deng Y., *et al*., Two-stage multichannel liquid–metal cooling system for thermal management of high-heat-flux-density chip array, *Energy Conversion and Management*, (2022), 259:115591

[19] Salehi A., *et al*., A numerical investigation of hydrogen impingement-effusion array jet for a heat sink cooling using solid/porous fins: A thermo-hydrodynamic analysis, *International Journal of Hydrogen Energy*, (2024), 52, pp. 381–396

[20] Ong KS., *et al*., Heat spreading and heat transfer coefficient with fin heat sink, *Applied Thermal Engineering*, (2017), 112, pp. 1638–1647

[21] Krishna Murthy K, Reddy KVK, Shaik AS, Badruddin IA, Kamangar S, Bashir MN, et al. Influence of rectangular micro inserts and micro chambers heat transfer characteristics of microchannel heat exchanger, *Case Studies in Thermal Engineering*, (2025), 65:105362

[22] Zhang Y., *et al*., Numerical research on the flow and heat transfer characteristics in the immersion jet cooling for servers, *Case Studies in Thermal Engineering*, (2024), 60:104748

Submitted: 13.01.2025

Revised: 14.02.2025

Accepted: 21.02.2025